Lasers in Eng., Vol. 44, pp. 277–288
Reprints available directly from the publisher
Photocopying permitted by license only

Study of Negative Side Wall Surface Roughness by Picosecond Photonic Impact Microdeposition

K.L. Yung, C.L Kang, Y. Xu and S.M. Ko*

Department of Industrial & Systems Engineering, The Hong Kong Polytechnic University, 11 Yuk Choi Road, Hing Hom, Kowloon, Hong Kong

Laser-induced forward transfer (LIFT) has been well studied for metals but for non-metals published work is scarce. With recent advance of picosecond laser, non-metal in the direction of photonic impact is giving more flexibility of deposition control, including the control of depositing position and the control of surface roughness of deposited structures. In view of producing microstructures in micromould demands high side wall surface quality that current LIFT or similar laser-assisted method could not achieve, this study introduces the control of size and shape of micropatches by adjusting the distance and environment of deposition using a picosecond laser beam. A new method is proposed to change the shape of each micropatch by using multiple photonic impacts rather than single impact to achieve high surface quality, which had never been reported. It enables production of microstructures where current single impact deposition methods have not yet been solved.

Keywords: Picosecond laser, micromould, laser induced forward transfer (LIFT), photonic impact forward transfer, side wall roughness, microdeposition, mechanical strength

1 INTRODUCTION

Limitations of laser-assisted deposition for producing microstructures mainly lie on the low mechanical strength caused by the dot by dot (for micropillars) or line by line (for microwalls) connection process, where the shapes of dots and lines are normally round. Other techniques have been studied. Jhaver *et*

*Corresponding author: E-mail: sm.ko@polyu.edu.hk

al. [1] studied the development of a novel technique - microplasma transferred arc (micro-PTA) for producing net-like metallic microstructures. Jerby *et al.* [2] used localized microwave heating (LMH) for melting bronze-based powder and its stepwise additive deposition to manufacture its rod using ceramic to support a tungsten electrode. They also used iron-based powder for magnetic fixation to provide a contactless means to hold the deposition powder instead of ceramic support.

Simulation of multi-layer and multi-material deposition using finite element (FE) simulation to study and predict distribution of temperature and stress, effect of deposition process parameters on them and modification mechanism of properties of deposition materials had also been carried out. Zhao *et al.* [3] carried out a three-dimensional (3-D) transient heat transfer simulation and investigated the thermal characters and effects of deposition directions on the thermal process for multi-layer deposition weld-based rapid prototyping. They optimized the deposition parameters and deposition direction through simulation.

There are many further studies of various forms of laser-induced forward transfer (LIFT) using different types of lasers for different purposes [4-9]. Amongst all the different approaches to LIFT, the picosecond laser as a matured industrial laser which can deliver highly concentrated pulse energy within a very short time to create an explosion with minimum melting is a good choice for LIFT. Previously, we studied the fabrication of micromoulds for producing plastic microneedle arrays using a picosecond laser [10]. We also studied experimentally forward transfer deposition of single dots [11] and microlines by connecting microdots [12] using a picosecond laser. The effects of deposition step-size on top surface roughness were studied and it was found that reducing spot size can reduce the surface roughness while the deposition thickness was also increased. This paper studies factors affecting the side wall roughness of deposited micropillars (the roughness of the top surface is not be discussed).

2 MICROPATCH SIZE CONTROL

2.1 Micropatch size control by changing laser target distance and laser power simultaneously

Previously, we have studied the effects of changing the spot size of deposited micropatches by adjusting the distance between laser and target of where the to be deposited materials locate. However, this would cause problems in the optimal usage of target materials. In addition, changing laser power amid the deposition process is not ideal for industrial manufacturing as power attenuation would reduce the energy efficiency.

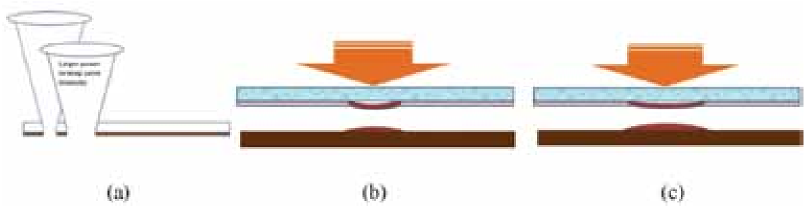

FIGURE 1
Schematic diagrams showing (a) micropatch size control in an inert gas environment by changing power and distance between laser and target together, (b) smaller power for larger distance and (c) larger power for closer distance.

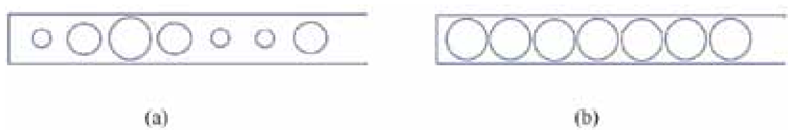

FIGURE 2
Schematic representations comparing target tapes resulting from changing the distance between the laser, the target and power together, against fixing the distance between laser and target when (a) changing the distance between the laser, the target and the laser power together, and (b) constant distance between the laser and the target.

Figure 1 illustrates the deposition of different spot size micropatches by varying the distance between laser and targets. Figure 2 illustrates the resulted difference on target tape by changing distance between target and laser. Changing distance between laser and target has to be accompanied by changing laser power at the same time, otherwise, the energy density on the target material would be different for different distances, causing incomplete material transfer or no material transfer at all. By comparing the target tapes resulted from changing distance between laser, target and power together, and changing the distance between target and substrate while keeping the distance between laser and target fixed, as shown in Figure 2, it is found that the efficiencies of material usages are dramatically different. Changing distance between laser and target and laser power together would result in non-uniform dot patterns on the target tapes. This reduced the material efficiency.

2.2 Micropatch shape and size control by changing deposition environment and target-substrate distance

The mechanisms of changing the size of micropatch by changing distance between target and substrate are illustrated in Figure. 5. In a vacuum, as the intensity of laser follows the Gaussian distribution that the intensity at the centre is the highest. This would exert more photonic energy at the centre and

FIGURE 3
Schematic illustration of shape differences affected by environment in the deposited micropatches in (a) a gas environment and (b) in a vacuum.

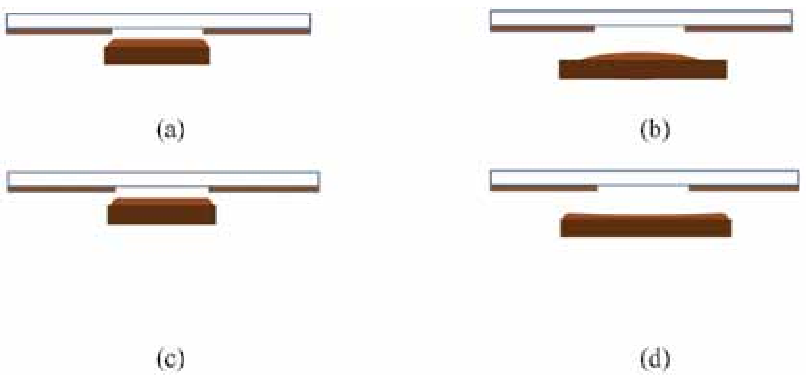

FIGURE 4
Schematic illustrations of micropatch size control by changing the distance between the target and the substrate showing that (a) a shorter distance between the target and the substrate resulted in a smaller micropatch on the substrate when deposited in an inert gas environment, (b) a longer distance between the target and the substrate resulted in a larger round shaped micropatch on the substrate when deposited in an inert gas environment, (c) a shorter distance between the target and the substrate resulted in a smaller micropatch on the substrate when deposited in a vacuum, and (d) a longer distance between the target and the substrate resulted in a larger concave micropatch on the substrate when deposited in a vacuum.

relatively less impact energy in surrounding area. The difference in impact energy distribution would result in more stretching deformation at the centre of a micropatch, resulting in thinner centre area after traveling a longer distance. While in inert gas, the gas pressure would force the soft micropatch to deform toward droplet shape, making the centre of micropatch thicker than surrounding area. In the same time, the stretching force on micropatch caused by air friction would result in larger micropatch when traveling longer distance before reaching the substrate. The disadvantages of depositing in vacuum are a higher cost in sealing and environmental control, and higher vaporization ratio of materials than in inert gas. To avoid this, depositing in inert gas and controlling the size of micropatches by changing distance between target and substrate, as shown in Figure 4(a) and Figure 4(b) are more practical and cost-efficient.

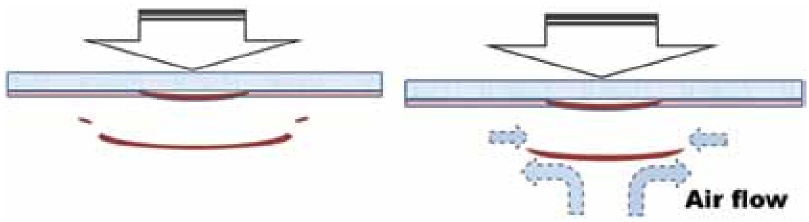

FIGURE 5
Schematic illustrations showing the size of the micropatch changing when deposited in (a) a vacuum and (b) in an inert gas environment.

3 VERTICAL AND NEGATIVE SIDE WALL ROUGHNESS AND SHAPE OF MICROPATCHES RESULTING FROM CONSTANT POWER IMPACT DEPOSITION

3.1 Vertical and negative side wall microstructures resulting from deposition when target-substrate distance is constant

Assuming that the round micropatch shape follows the shape of a sine function, then it can be represented as z, by

$$z(x) = a_i \sin\left[\left(\frac{x}{h_i}\right)\pi\right](0 \le x \le h_i) \quad (1)$$

When the distance between two micropatches is less than Δh_{min}, the two patches are connected and thus the part between $z(x=\Delta h_{min}/2)$ and $-z(x=\Delta h_{min}/2)$ is 100% continuous solid. The part outside this area is a series of disconnected bumps forming the rough side of the micropillar deposited.

The roughness average calculation equation is

$$Ra = \frac{1}{l}\int_0^l |Z(x)|\, dx \quad (2)$$

The surface roughness of the side wall of the microstructure as shown in Figure 6(a) is obtained from

$$Ra1 = \frac{1}{h_i}\int_0^{hi} |z(x)|\, dx = \frac{1}{h_i}\int_0^{hi} \left| a_i \sin\left(\left[\left(\frac{x}{h_i}\right)\right]\right)\right| dx = -\frac{2a_i}{} \cos\left(\left[\left(\frac{x}{h_i}\right)\right]\right)\Big|\left(x = \frac{\Delta h_{min}}{2} to \frac{h_i}{2}\right) \quad (3)$$

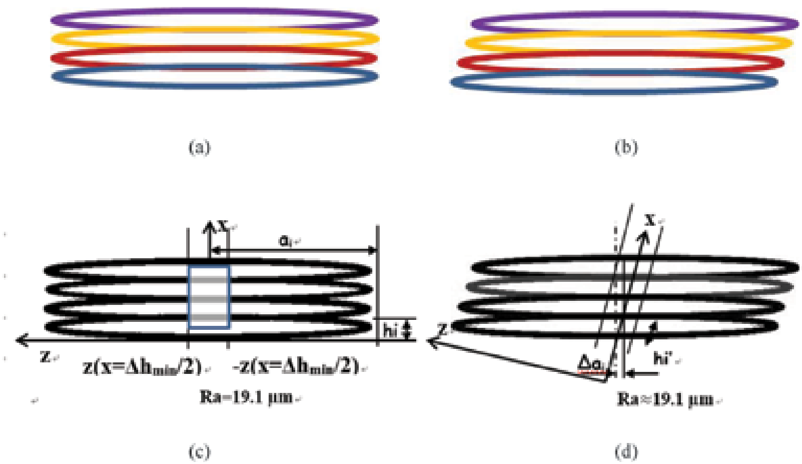

FIGURE 6
Schematic illustrations of the vertical side wall microstructures and surface roughness obtained when depositing in the same location continuously and keeping the target-substrate distance constant for the (a) vertical side wall, (b) negative side wall on one side and positive side wall on another side, (c) and (d) the respective parameters used for calculating the surface roughness.

When a_i=30 μm, h_i=30 nm and Δh_{min}=1 nm, we have Ra1=19.1 μm.

When using micropillars with high surface roughness, demoulding resistance would be extremely high, causing failure in demoulding in microinjection moulding. Although deformable material such as a shape memory alloy (SMA) could reduce the resistance a little, the overall performance is not comparable to those with high surface quality.

3.2 Negative side wall microstructure resulting from deposition by changing target-substrate distance slowly

By increasing the target-substrate distance slowly in a series of consecutive photonic impact depositions, negative side wall shaped microstructures can be formed, as shown in Figure 8(a) and Figure 8(b). The side wall roughness is directly related to the shape of the micropatches, as is evident from Figure 6 and Figure 7. The top surface would not be flat but would be concave in vacuum deposition, as shown in Figure 8(a) and dome-shaped in inert gas deposition, as shown in Figure 8(b).

3.3 Effects of side wall roughness on the strength of the microstructures produced

It is known that round-shaped micropatches would form porous microstructures with much less mechanical strength. At the same time, micropillars deposited by staggering round shaped micropatches together would not only show high sur-

FIGURE 7
Optical micrograph showing the vertical wall surface produced with layer-by-layer deposition of a polymer with a layer thickness of 200 μm.

(a) (b)

FIGURE 8
Schematic diagrams showing the predicted negative side wall shaped microstructures resulting from deposition in the same place repeatedly and changing the target-substrate distance slowly when deposited (a) in a vacuum and (b) in an inert gas environment.

face roughness. Its mechanical strength would also be severely deteriorated. Less mechanical strength would cause plastic deformation rather than elastic deformation, resulting in functional failure. The maximum stress, σ_{max}, is given by

$$\tilde{A}_{\max} = \frac{M}{I} \tag{4a}$$

and

$$\tilde{A}'_{\max} = \frac{M}{\mathrm{I}'} \tag{4b}$$

where I and I' are the moments of inertia of bars with cross-section diameters D and D', respectively, which are the moments of inertia for calculating the maximum stress in a micropillar of smooth and rough surface respectively. Now

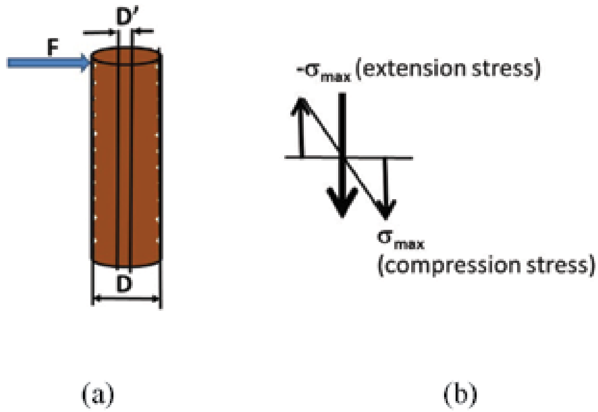

FIGURE 9
Schematic illustration giving the mechanical strength being weakened due to a non-smooth surface. (a) The dimension of micropillar and (b) the stress distribution at the root of the micropillar, where the maximum extension stress and maximum compression stress both happen at the surface of the continuous part. The diameter of continuous pillar is *D* for the micropillar with a smooth surface. The diameter of continuous pillar is *D'* for a micropillar with a rough surface.

$$I = \frac{D^3}{64} \tag{5a}$$

and

$$I' = \frac{D'^3}{64} \tag{5b}$$

As *D*>>D', then *I*>>I' so $?_{max}$>>$?'_{max}$. For the micropillar shown in Figure 6(a), *D'*=0.05*D* which leads to $?_{max}/?'_{max}$ =$(1/0.05)^3$=8000. Less maximum stress means higher mechanical strength of the micropillar produced. Moreover maximum stress means lower mechanical strength of the micropillar produced.

The above calculation showed that the side wall surface roughness of micropillar produced by deposition is critical to its mechanical strength. The round shape of deposited dots severely reduces the mechanical strength, which is critical to the application of microstructures. To produce micropillars using photonic impact deposition, reshaping the traditional spherical shaped micropatches is critical.

4 MICROPATCH SHAPE CONTROL USING MULTIPLE IMPACTS

The momentum and force of pushing materials forward comes from explosion like vaporization of materials. When laser pulse power is high as the pulse shown in

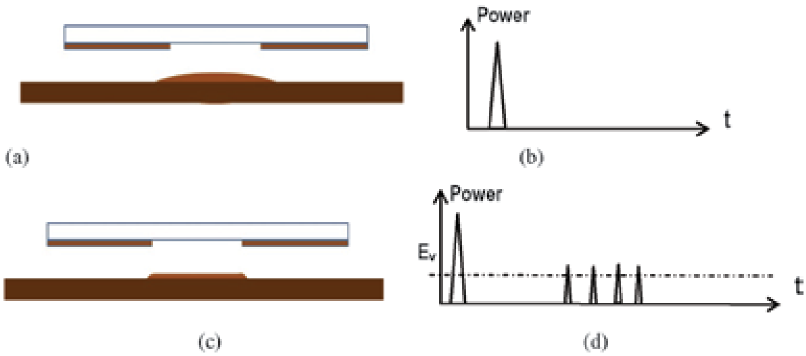

FIGURE 10
Illustrations and plots for the changing shapes of the micropatches by varying the number of impacts. (a) The shape of the micropatches tend to be round when deposited in an inert gas environment with single impact deposition, shown in (b), and (c) the shape of the micropatches can be flattened after multiple small impacts are added, shown in (d).

Figure 10(b), most of the energy goes to explosion effects, making thermal effects much less obvious comparing with those for materials breaking and moving.

When the laser pulse is lower as the 4 mini pulses shown in Figure 10(d), most energy goes to thermal effects, which is softening the material. The small explosive energy would deform the softened materials and making the micropatches flatter.

5 MICROSTRUCTURES RESULTING FROM MULTIPLE IMPACTS DEPOSITION

5.1 Deposited microstructure surface quality improvements by multiple impact deposition when keeping target-substrate distance constant

The surface roughness of micropillar shown in Figure 12(a) is 0. The surface roughness of micropillar shown in Figure 12 (b) can be calculated. According to the equation for roughness,

$$Ra2 = \frac{1}{l}\int_0^l |Z(x)|\,dx = \frac{h_i * \frac{a_i}{2}}{h_i^{'}} = \frac{h_i^2 \sin(15°)/2}{\sqrt{h_i^2 + \Delta h_i^2}} = 0.125 h_i \qquad (6)$$

Taking the same values used for microstructures shown in Figure 6, *hi*=30 nm and a_i=30 μm, the surface roughness of microstructures shown in Figure 12(b) is an Ra of 3.73 nm. This is much less than the 19.1 μm surface roughness of the microstructure deposited by single impact deposition, as shown in Figure 6.

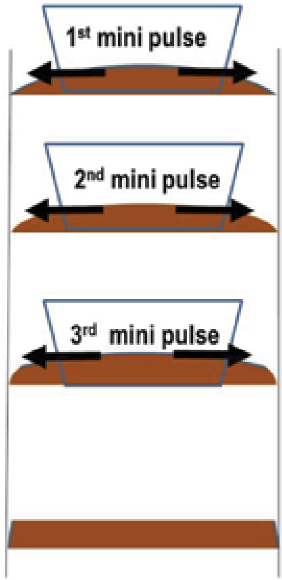

FIGURE 11
Schematic illustration showing the change in shape of the micropatches resulting from multiple mini-pulses.

5.2 Multiple impact deposition by changing target-substrate distance slowly

Similar to the structure shown in Figure 12(b), the strength and surface quality of micropillars with negative side wall, as shown in Figure 13, produced by multiple impacts deposition would also be in the same scale. This is much better than those produced by single impact deposition.

6 CONCLUSIONS

Changing the shape of micropatches deposited by picosecond laser photonic impact deposition by using multiple impact rather than single impact was proposed. Effects of the shape of the micropatches on side wall surface roughness and the mechanical strength of the micropillars deposited were analysed. It was found that the improvements to the shape of micropatches by using multiple impacts could improve the surface quality of the micropillars thousands fold, from 19.1 μm to 3.73 nm. Likewise mechanical strength would also be improved thousands fold. These improvements are critical to the fabrication of micropillars in micromoulds for microinjection moulding using metallic materials not suitable to be produced with microelectroforming.

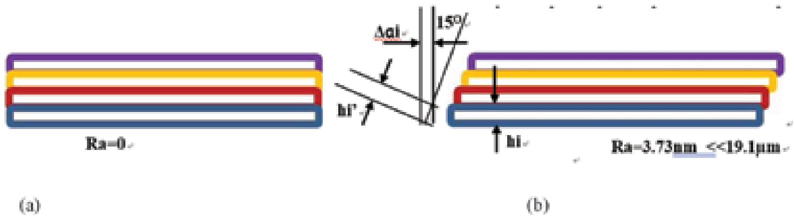

FIGURE 12
Schematic illustrations of the side wall micropillars obtained by depositing in the same location continuously and keeping the target-substrate distance constant using multiple impact pulses for each micropatch, as shown in Figure 6, on (a) the vertical side wall and (b) the negative side wall on one side and positive side wall on another side.

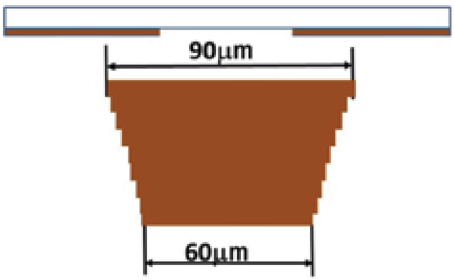

FIGURE 13
Illustration giving the surface roughness of the negative side wall shaped microstructures resulting from multiple impact deposition. Here, Ra=3.73 nm is much smaller than Ra=19.1 μm resulting from single impact deposition.

7 ACKNOWLEDGEMENTS

This research was supported by a fund from the Hong Kong Polytechnic University (A/C: G-YN83). The equipment was partially supported by a UGC fund (Ref. SEG_PolyU09).

REFERENCES

[1] Jhaver S., Jain N.K. and Paul C.P. Development of micro-plasma transferred arc (μ-PTA) wire deposition process for additive layer manufacturing application. *Journal of Materials Processing Technology* **214**(5) (2014), 1102-1110.
[2] Jerby E., Meir Y., Salzberg A., Aharoni E., Levy A., Torralba, J.P. and Cavallini, B. Incremental metal-powder solidification by localized microwave-heating and its potential for additive manufacturing. *Additive Manufacturing* **6** (2015), 53-66.
[3] Zhao H., Zhang G., Yin Z. and Wu L. A 3D dynamic analysis of thermal behavior during single-pass multi-layer weld-based rapid prototyping. *Journal of Materials and Processing Technology* **211**(3) (2011), 488-495.

[4] Eric B., Kim H., Auyeung R.C. and Pique A. Laser-induced Forward Transfer of Ag Nano-paste. *Journal of Visualized Experiments* **109** (2016), 53728.

[5] Papazoglou S. and Zergioti I., Laser induced forward transfer (LIFT) of nano-micro patterns for sensor applications. *Microelectronic Engineering* **182** (2017), 25-34.

[6] Klini A., Loukakos P.A., Gray D., Manousaki A. and Fotakis C. Laser Induced Forward transfer of metals by temporally shaped femtosecond laser pulses. *Optics Express* **16**(15) (2008), 11300-11309.

[7] Visser C.W., Pohl R., Sun C., Romer G.W., Huis in't Veld B. and Lohse D. Toward 3D printing of pure metals by laser-induced forward transfer. *Advanced Materials* **27**(27) (2015), 4087-4092.

[8] Serra P., Colina M. and Femandez-Pradas J.M. Preparation of functional DNA microarrays through laser–induced forward transfer. *Applied Physics Letters* **85**(9) (2004), 1639.

[9] [Shugaev M.V. and Bulgakova N.M. Thermodynamic and stress analysis of laser-induced forward transfer of metals. *Applied Physics A: Materials Science & Processing* **101**(1) (2010), 103-109.

[10] Yung K.L., Xu Y., Kang C.L., Liu H., Tam K.F., Ko S.M., Kwan F.Y. and Lee T.M.H. Sharp tipped plastic hollow microneedle array by microinjection moulding. *Journal of Micromechanics and Microengineering* **22**(1) (2012), 015016.

[11] Yung K.L, Kang C.L. and Xu Y. A study of pulse by pulse microscale patch transfer using picosecond laser. *International Journal of Engineering Research and Application* **6**(9) (2016), 55-58.

[12] Xu Y., Huang L.B., Yung K.L., Xie Y.C. and Lee T.M.H. Low cost fabrication of microelectrodes on plastic substrate of microbiochip. *Microsystem Technologies* **17** (3) (2011), 361-366.